Improved Optical Model Based on Region Segmentation for Single Image Haze Removal

Qieshi Zhang and Sei-ichiro Kamata

***Abstract*—In this paper, we propose a novel method to recovery the haze-free image based on the improved optical model with the single image based depth estimation. In this work, the objective transmission and distance transmission are present to improve the optical model for obtaining the haze-free image. Firstly, the color clustering method is used to segment the image into several regions by color similarity. Then, the graph-based segmentation is used to calculate the depth information. Next, the atmosphere light is estimated according to the distance transmission. And finally, the improved optical model is used to estimate the haze-free image. The experimental results show that our method is more effective and able to get better results than other single image based methods.**

***Index Terms*—Haze removal, image segmentation, single image, optical model.**

I. Introduction

Nowadays, the computer vision based technologies are widely used, however the quality of captured image influence the final effective strongly. In outdoors scenes, some natural elements influence the quality of captured image. Such as, haze, smoke, fog, rain, snow and other atmosphere factors. In our daily life, haze is the most common problem because of the atmosphere quality Fig. 1(a). So the haze removal technology Fig. 1(b) needs be studied to recovery clear image for satisfying the computer vision applications.

Usually, the haze influenced by different objects and different distance (we call it as the depth information) are different. So Narasimhan and Nayar [1]-[4] use the multi-image under different density of haze conditions to calculate the depth information. For these kinds of methods, they need capture the multi-image at same scene under different times with different atmosphere conditions. If the difference is little, the results will not accuracy. However, in many real applications, it's hard to get multi-image in same scene with this condition. So this limits the development and the practical application. Considering this short come, more and more researchers aim to use the single image to solve this. However, to obtain the depth information from single image is very difficult.

For solving this problem, in short recently, some single image based haze removal methods have been developed [5]-[8]. For single image, the depth information cannot be calculated directly, so the estimation methods are used with the optical model. Fattal [5] uses the Independent Component

(a) Hazy image (b) Our result
Fig. 1. Haze removal using a single image

Analysis (ICA) to estimate the transmission map. However, this method is hard to get idea result when the hazy is heavy. Also, if the ICA assumption not correct, it will get wrong result. Tan [6] calculates the maximization of local contrast to enhance the image, and then use the Markov random field (MRF) for haze removing. But this method didn't consider the atmosphere light, so sometimes it leads to over-enhanced of some regions, specially the sky region. Kratz and Nishino [7] proposed the probabilistic method for factorizing the hazy image and the MRF is used to estimate the energy to haze removal. This method can get clear result, but the vision effect is not natural. He *et al.* [8] propose a dark channel prior by analyzing many haze-free images. This prior of the haze-free image is close to black, and for hazy image become to bright. So it can be used to estimate the transmission map and the atmospheric light. For optimizing the transmission map, the soft matting [9] is used to instead of MRF. However, the calculation cost is expensive and for local bright or multi-light source cannot get idea results.

Consider the advantage and disadvantage of existing single image based methods. In this paper, an improved optical model with single image based depth estimation is used to analyze the hazy influenced image and hazy layer, respectively. Then use the color clustering method to segment the different objects (assumption different objectives have different colors). After that use the graph-based segmentation method to estimate the depth and calculate the atmosphere light in every region then decide the best one. Finally, use the improved optical model with the calculated parameters to estimate the haze-free image.

The remainder of this paper as follows: In Section 2, the improved optical model is introduced and analyzed. Then, the object transmission, distance transmission, and atmosphere light are estimated in Section 3. In Section 4, the results are compared with other up-to-data methods and discussed in detail. Finally, we conclude the advantage of proposed method and analyze the future works.

II. Improved Optical Model

Nowadays, the following image optical (degradation)

Manuscript received December 15, 2011; revised December 30, 2011.
The authors are with the Graduate School of Information, Production, and Systems (IPS), Waseda University, Kitakyushu, 808-0135, Japan. (e-mail: Q.Zhang@Akane.waseda.jp; e-mail: kam@waseda.jp).

model is mostly be used in previous haze removal methods [5]-[8]:

$$Y(x) = I(x)T(x) + A[1 - T(x)]. \quad (1)$$

Here $I(x)$ is the haze-free image, $Y(x)$ is the hazy image, A is the atmosphere light, and $T(x)$ is the transmission map where $T(x) = e^{-\beta d(x)}$. The β is the attenuation coefficient which assumed to be the uniform across the entire scene, d is the scene depth from the real object to observer, and x is the position of pixel. In the Equation (1), the first term is the direct attenuation and the second term is the influenced atmosphere light.

In previous methods, they usually estimate the $T(x)$ and A to calculate the haze-free image $I(x)$. However, by our analyzing, only use one transmission map $T(x)$ to estimate the haze-free image is not accuracy enough. Due to the influence of atmosphere, the light of objective become to weak and the light of sky become to bright. The captured image is composed with decay clear image and the enhanced atmosphere light image. So the observed image $Y(x)$ include the decay haze-free image $I(x)T(x)$ and hazy layer $A[1\text{-}T(x)]$ as Fig. 2 shows. In fact, the $T(x)$ of the first term in right hand is depend on element (color) of objects, because of different element have different diffuse reflectance and denote as $T_{obj}(x)$. The T of the second term in right hand is influenced with the distance, because it is the diffuse reflectance of atmosphere and denotes as $T_{dis}(x)$. Consider this difference; Equation (1) should be rewrite as:

$$Y(x) = I(x)T_{obj}(x) + A[1 - T_{dis}(x)]. \quad (2)$$

Based on this improvement, the haze removal problem is convert to A, $T_{obj}(x)$, and $T_{dis}(x)$ estimation problem from known single image $Y(x)$. However, the estimations are needed use the suitable segmentation and prior knowledge to obtain the accuracy values. The stage of the proposed optical model is show as Fig. 2. The Fig. 2(a) is the known hazy image, (c), (d), and (e) are the estimated transmission map by region segmentation. This is different with He *et al.*'s method [8]. In He *et al.*'s method, the transmission map (b) is calculated at first, and then optimizes it to get (e). Compare with the transmission map in [8], our objective transmission T_{dis} [Fig. 2(c)] shows more detail than (e). Not only this, the considered objective diffuse reflection makes the edge information more clear. Not only this, the distance transmission T_{obj} [Fig. 2(e)] effective to reflect the depth information to make the atmosphere influence estimation more accuracy.

III. Region Segmentation based Estimation for Debasing

As we known, the single image haze removal is an ill-posed problem. Because of the parameters are unknown and hard to estimate the original hazel-free image by the optical model exactly. Recently, He *et al.* [8] proposed a new approach by observing the dark channel statistical. He *et al.* optimize the dark channel as the transmission map to estimate the haze-free image. The dark channel is novel; however, this prior is not always correct. And the author never consider the diffidence of T_{obj} and T_{dis}, only simply assume them are equal. In the multi-light source situation, the atmosphere estimation is not always established. With the similar approach, other existing methods also use one transmission map to solve this problem simply. For obtaining more accuracy results, our method estimates the objective and distance transmission map by segmentation, respectively.

A. Objective Transmission Map (T_{obj}) Estimation

Considering the different objects have different diffuse reflection ability, so the object segmentation based analyze will help to obtaining the transmission map more accuracy. Due to the diffuse reflection is influenced by color of objects usually, not the distance or the whole shape of objects. Hence, we adopt the color clustering method to cluster the true color (24bits) image into k colors to reflect the color distribution. And then calculate the minimum of every pixel (min(R, G, B)) to get the transmission map [8].

The advantage of [8] is making the prior of haze free image. However, it needs be optimizing to get more accuracy transmission map for haze removing. Because of they never consider the influence of similarity and the difference with objects and colors. Here, we analyze the characteristic of objects in many images, and find that usually the closer colors of objects have similar diffuse reflection. So use the clustering method can get idea k colors image to reflect the objects distribution and then calculate the dark channel by pixel directly. For fixing the k, we test and analyze many images. From the experiment results, if the k is too large, this processing is no meaning and hard to show by 8-bit pixel; if the k is too small, the transmission map will have obvious contour to influence the result. So, in this research, the number of colors is set as k=256.

In this paper, the image-clustering algorithm, which described in [10] is used to in the color barycenter hexagon (CBH) model [11] to get idea segmentation result [Fig. 2(c)].

1) Clustering by K-means: Here the set of observations are the all pixels with the corresponding color information. Usually, the k initial points are selected random, but here for getting all kinds of color, the average distributed k points in CBH model are selected as the initial points. After that, the minimum distances of all pixels are calculated as [10] described. Finally, the 256 values color image can be obtained and mapping it into gray image.

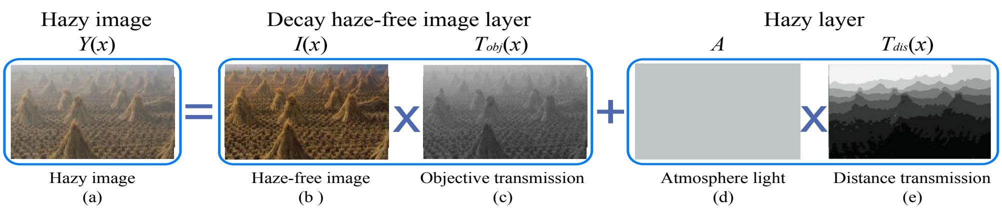

Fig. 2. Improved optical model

2) Color Descriptor in CBH Model

The CBH model is conveying the RGB color-to-color hexagon distribution for more accuracy observation. In the image processing field, RGB color space is widely used and it's a good choice for showing the relation of color. However, RGB color space not enough to describe the color feature and to cluster the color. By analyzing the relations of *R*, *G*, and *B* components, using the color triangle can easier to solve this problem. The three-dimensional (3D) RGB color space [Fig. 3(a)] is converted to a two-dimensional (2D) Polar Coordinate System (PCS) for creating the color triangle, as shown in Fig. 3(b). The conversion equations are as follows.

$$\begin{cases} \begin{bmatrix} \varphi_R \\ r_R \end{bmatrix} = \begin{bmatrix} 0 & 0 & 0 \\ 1 & 0 & 0 \end{bmatrix} \begin{bmatrix} R \\ G \\ B \end{bmatrix} + \begin{bmatrix} \frac{\pi}{2} \\ 0 \end{bmatrix} \\ \begin{bmatrix} \varphi_G \\ r_G \end{bmatrix} = \begin{bmatrix} 0 & 0 & 0 \\ 0 & 1 & 0 \end{bmatrix} \begin{bmatrix} R \\ G \\ B \end{bmatrix} + \begin{bmatrix} \frac{2\pi}{3} \\ 0 \end{bmatrix}. \\ \begin{bmatrix} \varphi_B \\ r_B \end{bmatrix} = \begin{bmatrix} 0 & 0 & 0 \\ 0 & 0 & 1 \end{bmatrix} \begin{bmatrix} R \\ G \\ B \end{bmatrix} + \begin{bmatrix} \frac{5\pi}{3} \\ 0 \end{bmatrix} \end{cases} \quad (3)$$

Here, *R*, *G*, and *B* are the color components of the RGB color space, and (φ_R, r_R), (φ_G, r_G), and (φ_B, r_B) are the coordinates in PCS. The color triangle is created as follows:

1) A standard 2D PCS is created (φ, r), where φ is the angular coordinate, and *r* is the radial coordinate $(\varphi \in [0, 2\pi), r \in [0, 255])$ [Fig. 3(b)]. In Fig. 3(b), r_R, r_G, and r_B are the color vectors, respectively.
2) Three color vectors are used to reflect *R*, *G*, and *B* with the range [0, 255] and alternate $\pi/3$, respectively.

$$\begin{cases} \text{R Component: } \varphi_R = \pi/2, \quad r_R \in [0,255] \\ \text{G Component: } \varphi_G = 2\pi/3, \quad r_G \in [0,255]. \\ \text{B Component: } \varphi_B = 5\pi/3, \quad r_B \in [0,255] \end{cases} \quad (4)$$

3) The three apexes are connected to create the color triangle.

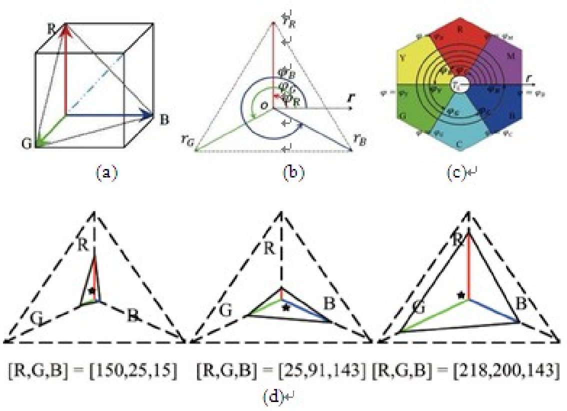

Fig. 3. Color triangle. (a) RGB color cube. (b) RGB color triangle. (c) CBH model. (d) Example of color triangle shape with different color

After the previous steps, the color triangle can be created, as shown in Fig. 3(b). The shape of the triangles is changeable for different *R*, *G*, and *B* combinations. As one combination only reflects one color, the color triangle only has one shape as well. For example, Fig. 3(d) shows three groups of *R*, *G*, and *B* components and their corresponding color triangles. In this example, changes in *R*, *G*, and *B* values do not mater the main structures are still unmodified (the origin *O*, and the directions of *R*, *G*, and *B* components are fixed). If *R*, *G*, and *B* equal the maximum value 255, the triangle will be the same as the main color triangle; else if *R*, *G*, and *B* equal the minimum value 0, the triangle will become one point and show in origin *O* of the main color triangle. Color information can be analyzed more clearly and easily based on the shape of the color triangle. The points of the 3D RGB color space are converted based on the conversion equation into several color triangles for further analysis.

The created color triangle, which described above cannot be used directly. However, analysis of the direction of the main color component finds the barycenter to reflect the color feature more accurately and intuitively. The barycenter $(\varphi_{Barycenter}, r_{Barycenter})$ is calculated in PCS:

$$\begin{cases} \varphi_{Barycenter} = \frac{1}{3}(\varphi_R + \varphi_G + \varphi_B) \\ r_{Barycenter} = \frac{1}{3}(r_R + r_G + r_B) \end{cases}. \quad (5)$$

One color triangle has one barycenter, and all barycenter are shown as a hexagon region [Fig. 3(c)]. This hexagon region shows the color feature of the image, and it is divided into seven regions, namely, M (Magenta), R (Red), Y (Yellow), G (Green), C (Cyan), B (Blue), and L (Luminance, achromatic) regions, which indicate the seven main colors. Observing the relationship between color and its corresponding barycenter position in the color triangle, closer *R*, *G*, and *B* components, small or large, only reflects the luminance information (weak color information). *R*, *G*, and *B* with close values do not reflect color feature. As such, the barycenter of the corresponding color triangles is located in a circular region (*L* region).

Based on the CBH model, the color feature can be described more accuracy than RBG color space. And we set the initial points of *K*-means as (φ_i, r_j), where $i = \{0, \pi/18, \pi/9, \cdots, 2\pi\}$ and $j = \{0, 10, 20, \cdots, 80, 85\}$. Then use these points to cluster by *K*-means.

3.3 Dark Channel

After the clustering, the quantized color image will be got as Y_k and the corresponding *R*, *G*, and *B* values as Y_{k_r}, Y_{k_g}, and Y_{k_b}. Then calculate the dark value of every pixel with the *R*, *G*, and *B* values. The objective transmission map is calculated by the following equation:

$$T_{obj}(x) = \min\left[Y_{k_r}(x),\ Y_{k_g}(x),\ Y_{k_b}(x)\right], \quad (6)$$

where Y_k is the quantized image, *x* is the pixel and *r*, *g*, and *b* mean the red, green, and blue color channel, respectively. Then the objective transmission T_{obj} can be shown as Fig. 2(c). Based on this transmission map with simple atmosphere, the preliminary haze removal image can be got. Though the removal effect is obviously, the detail information is not clear and need be improved. So in the following sections, the distance transmission map and atmosphere light will be studied to improve the haze removal result.

B. Distance Transmission Map (T_{dis}) Estimation

In He *et al.*'s method [8], the authors use the patch to segment the image with the regular structure. However, the regular patches cannot show the best distribution of natural image, so in this paper we use region to instead of the patch to estimate the depth of image. In this stage, the graph-based segmentation method [12] is used for segmenting. And the parameters include the smooth factor σ, thresholding constant T_h, and minimum distance *min*, which set as $\sigma = 0.5$, $T_h = 50$, and *min*=50. After that, using Equation (6) for every regions to obtain the depth image (this is certified by [8]).

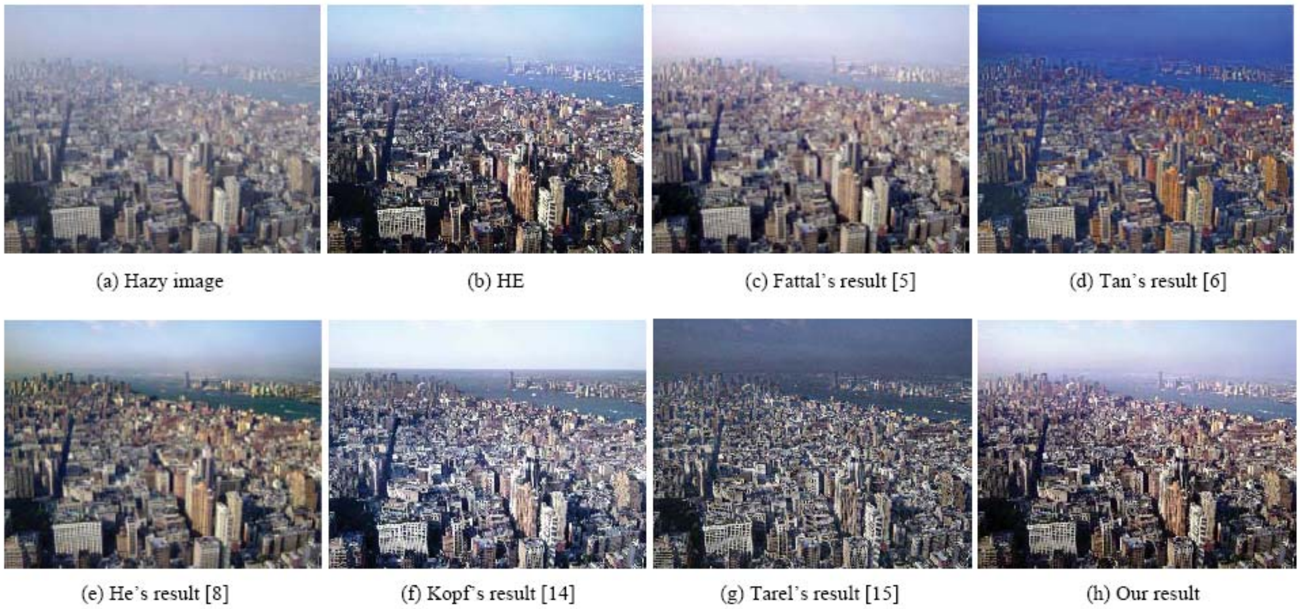

Fig. 4. Haze removal methods comparison 1

C. Atmosphere Light A Estimation

In many previous works, the atmosphere light *A* is estimate from the hazy image directly, after [8] estimate *A* from dark channel and then calculate the *A* from same pixels in hazy image. In our research, after the distance transmission map estimated, several depth regions will be got. Here we choose the deepest three region and then select the 10% brighter pixels in every regions. After that, calculate the same pixels in hazy image and choose the brightest one as the atmosphere light *A*. This selection method can obtain the atmosphere light automatic and overcome the multi-light source influence.

D. Recovering the Haze-free Image

With the objective transmission, distance transmission map and the atmosphere light, we can calculate the haze-fee image by Equation (2). But sometimes, the calculated T_{obj} value of pixel is close to zero, direct use it will let the recovered pixel become to infinite. Therefore, we use the minimum transmission value T_0 to limit the lower bound. So the final recovered haze-free image *I*(*x*) as following:

$$I(x) = \frac{Y(x) - A[1 - T_{dis}(x)]}{\max(T_{obj}(x),\ T_0)}. \tag{7}$$

The typical value of T_0 refer [8] to set as 0.1. After the recovering, to get more well vision effect, a contract enhancement method [13] is used.

IV. Experimental Results and Discussion

In order to compare the effective of our method with other methods, many natural hazy images are tested. In the experimental part, the same hazy images are widely tested in previous works [5]-[8], [14]-[16]. Compared with the optical model based methods, the advantage of the proposed method is the objective and distance being considered which have different diffuse reflection. Based on this, the objective and distance transmission map is calculated for obtaining more accuracy estimation. In this section, four images are used for comparing.

Observing the four test images with the results of all referred methods, the local contrast enhancement based Tan's [6] result always looks dark and too many details are lost, but it shows the best perception of distance. Tarel's result [15] is a little dark and can get ideal effect in near region, but the effect of far region is bad. For the whole image, the result of histogram equalization (HE) can be acceptable, but in some situations the far region is not good. Compare with all tested methods, Fattal's [5], He *et al.*'s [8], Kopf's [14], and proposed method are acceptable, following we will discuss them in detail.

In Fig. 4, one city image is used for comparing. For the whole image comparison, Fattal's [5], He *et al.*'s [8], and the proposed method are look same and can keep many details. The Kopf's method [14] is a little bright but the sky region is not good enough and the cloud region is missing. Compare the Fig. 4(c), (e), and (h), the far region in He *et al.*'s [8] result is the best, but the whole image looks not natural than others (expect Tan's [6] and Tarel's [15] results which looks too dark).

In Fig. 5, another city's image is used to compare. Fattal's method [5] is clear but the contract is not good, and some sky regions are missed. He *et al.*'s [8] result is a little dark and the far region is a little dark. Compare with other results, the Kopf's [14] method and proposed method can keep the details and get ideal effect no matter the near or far region with natural vision.

Figs. 6 and 7 show the nature image with mountain. In these figures, the sky region of He *et al.*'s [8] result looks best but the global effect is dark and many details of forest are missing. Fattal's [5] effect looks natural, but also cannot keep the details than Kopf's [14] and proposed method. Compared with other results, the proposed looks more natural and keeps more details.

In addition the subjective comparison, here perform the contrast preservation evaluation by the measure of Aydin *et al.*'s [17] which called as independent image quality assessment (IQA). By comparing the original hazy image with the haze-free images which restored by different methods, the quality measure finds the regions where the contrast has been amplified (the blue pixels in [17]) and regions where the contrast has been lost (green pixels in [17]), and more details can refer to their paper. Table 1 displays the average ratio with IQA measure on different methods. Compared with the other methods our method is able to amplify better the original contrast while the loss of details is reduced. segmenting need be further studied, and the estimation of distance transmission map is not accuracy enough. The parameters setting needs be improved and automatic select the best one. Based on these two improvements, the haze removal result should be become well.

TABLE I: AVERAGE SCORE OF IQA MEASURE BY [17]

Method	HE	Fattal's [5]	Tan's [6]	Kratz's [7]	He's [8]	Kopf's [14]	Tarel's [15]	Proposed
Amplified	1.24	0.36	0.14	0.37	1.43	1.52	0.23	1.59
Lost	1.82	1.98	2.61	2.46	2.21	1.39	1.75	1.37

V. CONCLUSIONS AND FUTURE WORKS

In this paper, an object and distance transmission map considered optical model is proposed. The advantages of the proposed method include three points:

1) Our method is based on color and region segmentation to calculate the object and distance transmission.
2) The proposed method can get more ideal result with more details.
3) This method can overcome the multi-light source influence.

However, how to decide the color number for objects

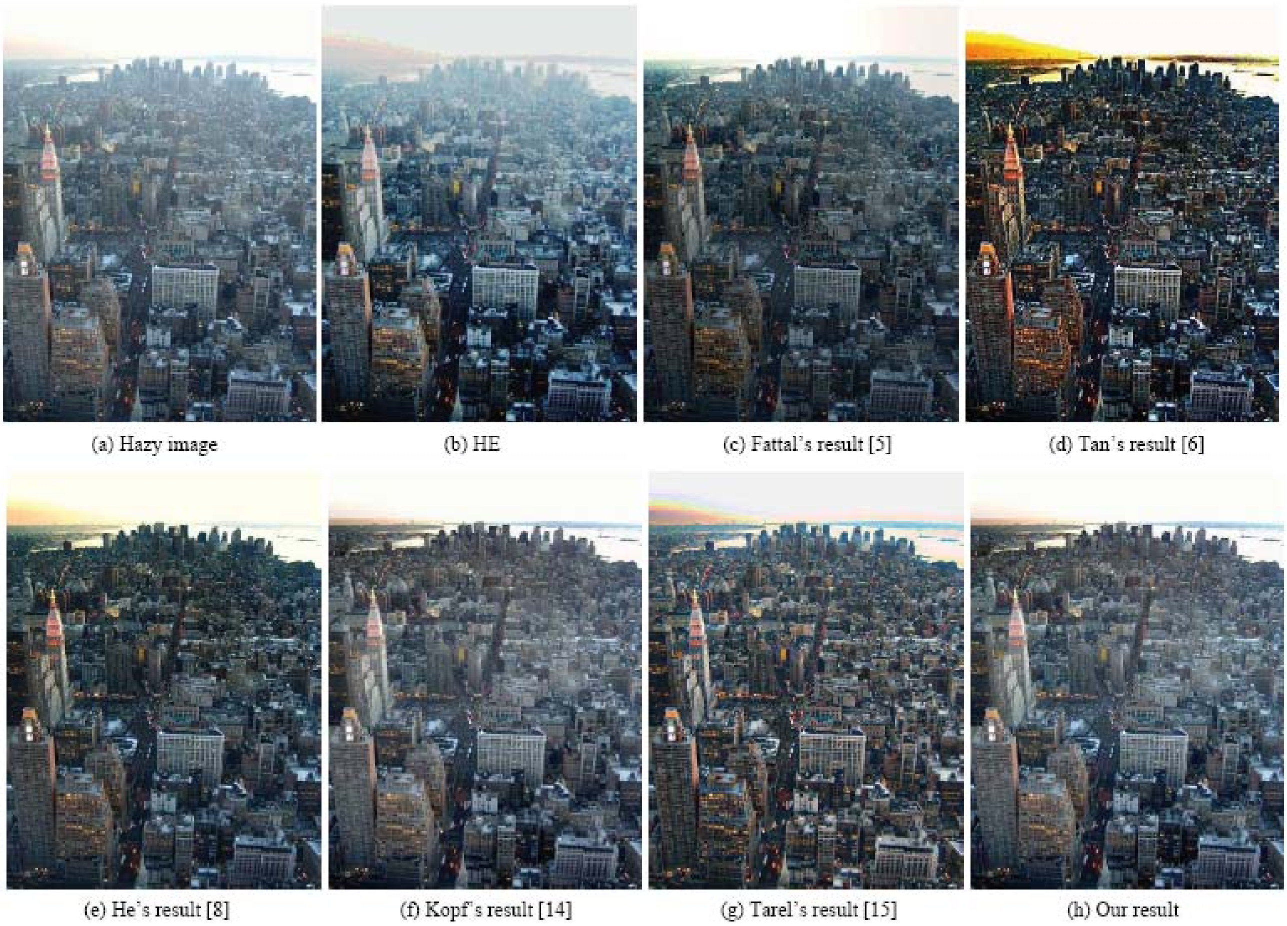

(a) Hazy image (b) HE (c) Fattal's result [5] (d) Tan's result [6]

(e) He's result [8] (f) Kopf's result [14] (g) Tarel's result [15] (h) Our result

Fig. 5. Haze removal methods comparison 2

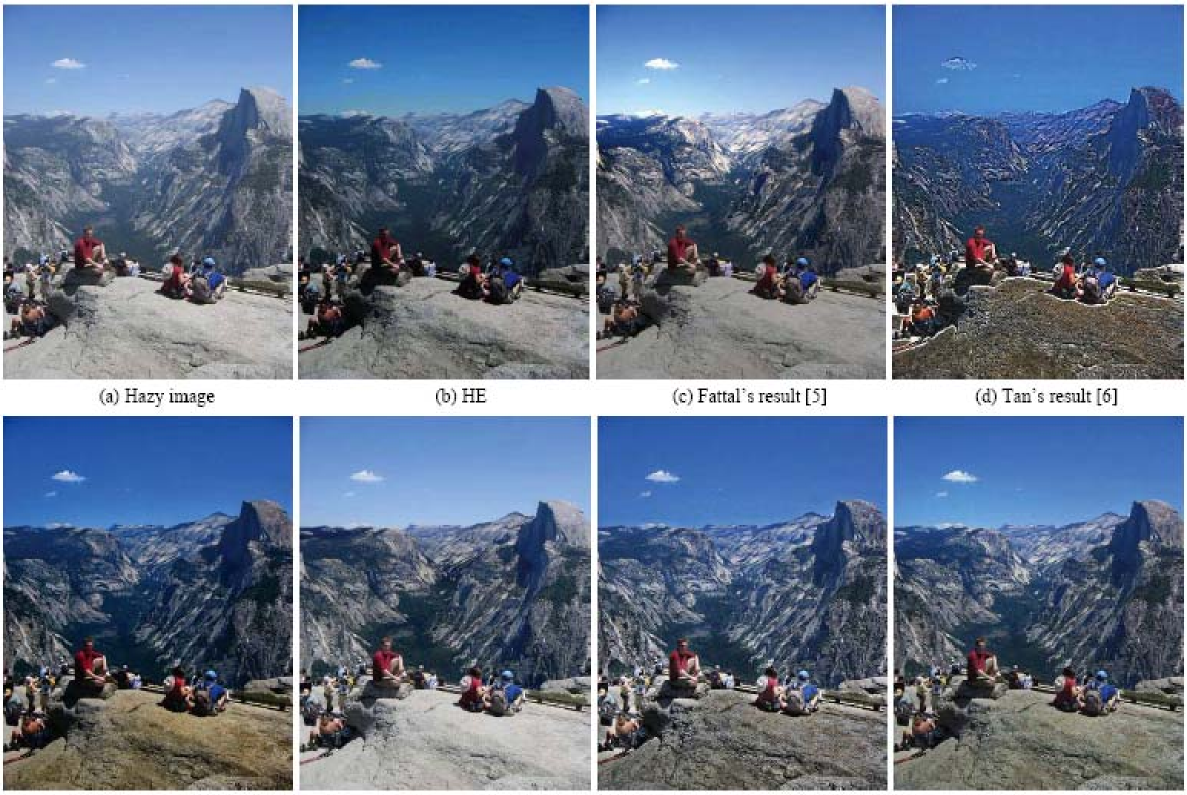

(a) Hazy image (b) HE (c) Fattal's result [5] (d) Tan's result [6]

(e) He's result [8] (f) Kopf's result [14] (g) Tarel's result [15] (h) Our result

Fig. 6. Haze removal methods comparison 3

(a) Hazy image (b) HE (c) Fattal's result [5] (d) Tan's result [6]

(e) He's result [8] (f) Kopf's result [14] (g) Tarel's result [15] (h) Our result

Fig. 7. Haze removal methods comparison 4

REFERENCES

[1] S. K. Nayar and S.G. Narasimhan, "Vision in bad weather," *IEEE Int'l Conf. on Computer Vision and Pattern Recognition* (CVPR), vol. 2, pp. 820–827, 1999.

[2] S.G. Narasimhan and S.K. Nayar, "Chromatic framework for vision in bad weather," *IEEE Int'l Conf. on Computer Vision and Pattern Recognition* (CVPR), vol. 1, pp. 598–605, 2000.

[3] S.G. Narasimhan and S.K. Nayar, "Vision and the atmosphere," *Int'l J. of Computer Vision*, vol. 48, pp. 233254, 2002.

[4] S.G. Narasimhan and S.K. Nayar, "Contrast restoration of weather degraded images," *IEEE Trans. on Pattern Analysis and Machine Intelligence* (T-PAMI), vol. 25, no. 6, pp. 713–724, 2003.

[5] R. Fattal, "Single image dehazingr," *ACM SIGGRAPH*, pp. 1956–1963, 2008.

[6] R.T. Tan, "Visibility in bad weather from a single image," *IEEE Computer Vision and Pattern Recognition* (CVPR), pp. 1–8, 2008.

[7] L. Kratz and K. Nishino, "Factorizing scene albedo and depth from a single foggy image," *IEEE Int'l Conf. on Computer Vision* (ICCV), pp. 1701–1708, 2009.

[8] K. He, J. Sun, and X. Tang, "Single image haze removal using dark channel prior," *IEEE Computer Vision and Pattern Recognition* (CVPR), pp. 1956–1963, 2009.

[9] A. Levin, D. Lischinski, and Y. Weiss, "A closed form solution to natural image matting," *IEEE Int'l Conf. on Computer Vision and Pattern Recognition* (CVPR), vol. 1, pp. 61–68, 2006.

[10] T. Kanungo, D.M. Mount, N.S. Netanyahu, C.D. Piatko, R. Silverman, and A.Y. Wu, "An efficient k-means clustering algorithm: Analysis and implementation," *IEEE Trans. on Pattern Analysis and Machine Intelligence* (TPAMI), vol. 24, pp. 881–892, 2002.

[11] Q. Zhang and S. Kamata, "Automatic road sign detection method based on color barycenters hexagon model," *Int'l Conf. on Pattern Recognition* (ICPR), pp. 1–8, 2008.

[12] F. Felzenszwalb and D.P. Huttenlocher, "Efficient graph-based image segmentation," *Int'l J. of Computer Vision*, vol. 59, pp. 167–181, 2004.

[13] Q. Zhang, H. Inaba, and S. Kamata, "Adaptive histogram analysis for image enhancement," *Pacific-Rim Symp. on Image and Video Technology* (PSIVT), pp. 408–413, 2010.

[14] J. Kopf, B. Neubert, B. Chen, M. Cohen, D. Cohen-Or, O. Deussen, M. Uyttendaele, and D. Lischinski, "Deep photo: Model-based photograph enhancement and viewing," *ACM Trans. on Graphics* (TOG), vol. 27, no. 5, pp. 116:1–116:10, 2008.

[15] J. Tarel and N. Hautiere, "Fast visibility restoration from a single color or gray level image," *Int'l Conf. on Computer Vision* (ICCV), pp. 2201–2208, 2009.

[16] C. Ancuti, C. Ancuti, and P. Bekaert, "Effective single image dehazing by fusion," *Int'l Conf. on Image Processing* (ICIP), pp. 3541–3544, 2010.

[17] T. Aydin, R. Mantiuk, K. Myszkowski, and H. Seidel, "Dynamic range independent image quality assessment," *ACM Trans. on Graphics* (TOG), vol. 27, pp. 69:1–69:10, 2008.

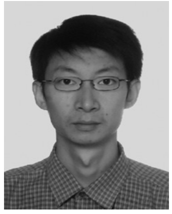

Qieshi Zhang is a Ph.D student of the Graduate School of Information, Production and Systems, Waseda University, Japan, where he received the M.S. degree in 2009. He received the B.E. degree major in Automation and minor in Computer and Application from the Faculty of Automation and Information Engineering, Xian University of Technology, China in 2004. From 2004 to 2006, he was an assistant engineer of the Department of Mechanical Electronically Technology in Xi'an Siyuan University, China. From 2009 to 2010, he was a teaching assistant in the Graduate School of Information, Production and Systems, Waseda University. Now he is Research Fellow of the Japan Society for the Promotion of Science (JSPS). His current research interests are in image processing, image compression, image detection, image enhancement, pattern recognition, and machine learning. Mr. Zhang is a student member of the IEEE and IEICE.

Sei-ichiro Kamata received the M.S. degree in computer science from Kyushu University, Fukuoka, Japan, in 1985, and the Doctor of Computer Science, Kyushu Institute of Technology, Kitakyushu, Japan, in 1995. From 1985 to 1988, he was with NEC, Ltd., Kawasaki, Japan. In 1988, he joined the faculty at Kyushu Institute of Technology. From 1996 to 2001, he has been an associate professor in the Department of Intelligent System, Graduate School of Information Science and Electrical Engineering, Kyushu University. Since 2003, he has been a professor in the Graduate School of Information, Production and Systems, Waseda University. In 1990 and 1994, he was a Visiting Researcher at the University of Maine, Orono. His research interests include image processing, pattern recognition, image compression, space-filling curve, and fractal. Dr. Kamata is a member of the IEEE, the IEICE and the ITE in Japan.